Dimerlike smectic-*A* and -*C* phases in highly fluorinated thermotropic liquid crystals

Thomas P. Rieker[1] and Eugene P. Janulis[2]
[1]*Sandia National Laboratories, P.O. Box 5800, Albuquerque, New Mexico 87185-1349*
[2]*3M Corporate Research Laboratories, St. Paul, Minnesota 55144-1000*
(Received 6 June 1994)

X-ray scattering studies on a homologous series of thermotropic liquid crystals with one tail perfluorinated reveal that the smectic layer thickness depends only on the length of the fluorocarbon tail. Density measurements in combination with the x-ray results show that the average cross-sectional area per molecule, parallel to the smectic layers, depends only on the length of the hydrocarbon tail. These experimental results lead to a model in which steric interactions drive antiparallel alignment of nearest neighbors in the smectic-*A* and -*C* phases. These unique dimerlike phases have a layer spacing comparable to the length of the molecules, demonstrate registration of nearest neighbors along their lengths, and exhibit ferroelectric switching in the chiral smectic-*C* phase.

PACS number(s): 61.10.−i, 61.30.Eb

I. INTRODUCTION

In this paper we report the discovery of unique dimerlike smectic-*A* (Sm-*A*) and smectic-*C* (Sm-*C*) phases of a class of rod-shaped, liquid-crystal-forming molecules having a perfluoroalkyl tail on one end of a rigid aromatic core and a hydroalkyl tail on the other. These materials present a unique system with sterically and chemically different ends. They exhibit a stronger propensity to form smectic phases than their hydrocarbon analogs and demonstrate unusual textures when viewed under crossed polarizers. Recently, a large number of such thermotropic liquid crystals have been synthesized [1–4] and evaluated for use in display devices.

Here we present structural studies for the 5-*n*-alkyl-2[4-*n*-(1,1-dihydroperfluoroalkoxy)phenyl]pyrimidine homologous series (Table I). In this homologous series both the hydrocarbon ($n|7$) and fluorocarbon ($10|m$) tail lengths are independently varied. These materials demonstrate the isotropic–Sm-*A*–Sm-*C* phase sequence. The Sm-*A* and Sm-*C* are layered phases in which the long axes of the molecules are aligned parallel to (Sm-*A*) or tilted (Sm-*C*) with respect to the normal of the smectic layers. Optically determined director tilt angles in the Sm-*C* phase of this homologous series will be reported at a later date. Ferroelectric switching is observed in the Sm-*C** phase in all homologs when a chiral dopant is added [5].

In the Sm-*A* and Sm-*C* phases the homologs in Table I exhibit the following structural properties: The smectic layer thickness depends only on the length of the fluorocarbon tail, while the average cross-sectional area per molecule depends only on the length of the hydrocarbon tail. This interesting response to changing molecular length indicates that the molecules are organized into a network of antiparallel pairs, i.e., with fluorocarbon and hydrocarbon moieties adjacent, such that the hydrocarbon tails do not contribute to the smectic layer spacing. Steric interactions dominate the amphiphilic interactions, tending to segregate the fluorocarbon and hydrocarbon tails.

II. EXPERIMENT

Aligned homeotropic samples were prepared on microscope slides cleaned with acetone. The substrates were placed on a hot plate and the liquid crystal melted and allowed to spread in the isotropic phase. The samples were then quickly transferred to a preheated single-stage scattering oven (stability $\approx \pm 50m$°C, T_{max} 115°C) in order to maintain the smectic phase. We found that the thin sample films broke up into droplets when cooled to the crystal phase and reheated. This flow-thinning technique produced a homeotropically aligned film approximately 20 μm thick (three samples were measured, using

TABLE I. Structure of the 5-*n*-alkyl-2-[4-*n*-(1,1-dihydroperfluoroalkoxy)phenyl]pyrimidine homologous series. For brevity, the homologs are referred to as $m|n$ where m (n) is the number of carbons in the hydrocarbon (fluorocarbon) tail. Phase transition temperatures (°C) for the various homologs were determined by differential scanning calorimetry, cooling from the isotropic phase at 5°C/min. All phases are also observed upon heating except for the Sm-*C* phase of 10|3 (monotropic). The liquid crystal phases were identified by polarized optical light microscopy. The identification of the smectic-*C* phase was confined by the observation of ferroelectric switching in chirally doped samples.

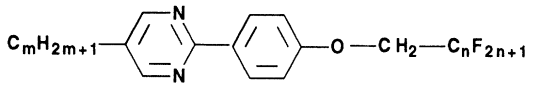

$m\|n$	X	Sm-*C*	Sm-*A*	I
6|7	50°C	56	133
7|7	54	67	125
8|7	71	80	117
9|7	71	85	112
10|7	75	87	104
10|5	47	73	84
10|3	36	52	64

a Zeiss light sectioning microscope) with a nearly uniform thickness over a 1×2 cm^2 area.

X-ray scattering experiments were conducted on a two-circle diffractometer with a rotating anode (Rigaku RU-300) Cu $K\alpha$ source, a bent graphite monochromator, slit collimation, and a Bicron scintillation detector. The x-ray spot size at the sample position was 0.275×2.0 mm^2 in cross section. The instrument resolution was 0.066°, full width at half height (FWHH), of a 2θ scan through the main beam.

Our scattering geometry was such that the samples were oriented normal to the floor and to the scattering plane of the instrument. With the detector in the main beam ($2\theta=0°$) and the sample just out of it, the plane of the substrate was oriented parallel to the beam with the diffractometer θ axis centered in the plane of the substrate. Alignment was completed by translating the sample normal to the beam until the beam intensity was halved. The detector (2θ) and sample (θ) orientations were scanned independently in order to locate and maximize the intensity of the (001) Bragg peak. At maximum intensity, θ was reset to $\frac{1}{2}$ of $2\theta_{\text{Bragg}}$. The samples were heated to just below the smectic-A to isotropic phase transition (temperature limited by the scattering oven) and held there for 15 min in order to stabilize the system. Data were collected as θ and 2θ scans (step sizes of 0.0125° and 0.025°) as the samples were cooled from the Sm-A to the crystal phase.

Density measurements were made by pycnometry using 20 μl capillary tubes heated to the Sm-A to Sm-C phase transition temperature in a single stage oven. A wire plunger was employed to compensate for material shrinkage as samples were cooled from the isotropic phase. The high degree of fluorination leads to densities $\sim$20–50% higher than for comparable hydrocarbon analogs [6].

III. RESULTS

The smectic layer spacing as a function of temperature for the individual homologs is shown in Fig. 1. All samples studied had monochromatorlike alignment with $0.04°\leq \text{FWHH}_{(001)}\leq 0.06°$, which is less than the instrument resolution (FWHH=0.066°), and a θ mosaic of 0.11° (FWHH). Higher order reflections were observed in all samples. The ratios $I_{(002)}/I_{(001)}$ and $I_{(003)}/I_{(001)}$ for individual homologs remained constant as the sample temperature was varied. The FWHH and symmetry of the observed Bragg peaks did not change with decreasing temperature, indicating suppression of layer fluctuations [7].

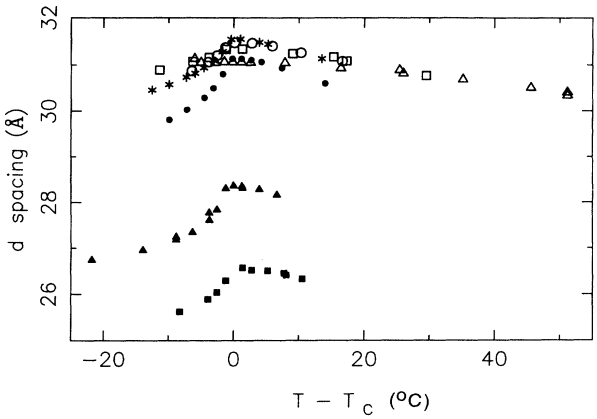

FIG. 1. Smectic-A and -C layer spacing as a function of temperature for the homologs in Table I. Changing hydrocarbon tail length: Δ, 6|7; □, 7|7; ○, 8|7; ∗, 9|7; ●, 10|7. Changing fluorocarbon tail length: ■, 10|3; ▲, 10|5; ●, 10|7.

The cross-sectional area per molecule was determined by combining the density and layer spacing data. Table II provides a summary of the pertinent experimental data. The average cross-sectional area per molecule vs molecular length for the homologs is plotted in Fig. 2.

IV. DISCUSSION

The layer spacing at the Sm-A to Sm-C phase transition is (1) *strongly dependent on the length of the fluorocarbon tail* (10|n homologs, Fig. 1); (2) *nearly independent of the hydrocarbon tail length* (m|7 homologs, Fig. 1) even though the molecular length varies by 20% (Table II). Furthermore, as the hydrocarbon tail length increases, this system maintains a constant layer spacing at the expense of increasing the average cross-sectional area per molecule (Table II and Fig. 2). In all cases the smectic layer spacing at the Sm-A and Sm-C phase transition

TABLE II. Summary of pertinent x-ray scattering and density data: Sm-A to Sm-C transition temperature (T_{AC}), smectic layer spacing at the Sm-A to Sm-C phase transition (d_{AC}), molecular length (l) (as calculated for the lowest energy conformation, using MOPAC [6]), density, and cross-sectional area per molecule for the various homologs.

$m\|n$	T_{AC} (°C)	d_{AC} (Å)	l (Å)	Density (g/cm^3)	Area per molecule (Å^2)
6|7	≈59.0(2)	31.1(2)	30.1(2)	1.46(±3%)	23.4(±4%)
7|7	70.0	31.4	31.3	1.45	23.8
8|7	82.8	31.5	32.7	1.40	25.2
9|7	86.4	31.6	33.9	1.37	26.3
10|7	87.9	31.2	35.3	1.39	26.8
10|5	75.2	28.5	32.6	1.31	26.5
10|3	53.4	26.6	30.0	1.23	25.2

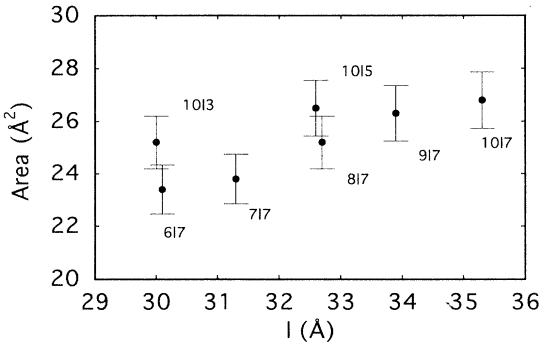

FIG. 2. Cross-sectional area per molecule vs molecular length. For increasing hydrocarbon tail length with fixed fluorocarbon tail length ($m|7$, $m=6,7,8,9,10$) the long range structure maintains a constant layer spacing at the expense of increasing the area per molecule. The cross-sectional areas of polytetrafluoroethylene (PTFE) and polyethylene (PE) are 28 and 22 Å^2, respectively [7].

(d_{AC}) is comparable to the molecular length (Table II).

The experimental facts suggest the formation of a long range network, normal to the smectic layers, of fluorinated tails and aromatic cores in which the smectic layer spacing is determined *independent of the length of the hydrocarbon tails* [Fig. 3(a)]. The parallel packing of neighboring molecules [like adjacent tails; see Figs. 3(b) and 3(c)], is excluded since the length of the hydrocarbon tails would necessarily contribute to the smectic layer spacing. We rule out interdigitated structures by the observation of ferroelectric switching in the Sm-C^* phase in chiral doped mixtures; i.e., this system demonstrates a low reorientational viscosity comparable to other Sm-C^* phases. We propose that neighboring molecules within a smectic layer are aligned, on average, in an antiparallel manner and are registered relative to one another along their lengths [Figs. 3(a) and 3(d)]. Probable local in-plane structures are square [Fig. 3(e)] or hexagonal [Fig. 3(b)] arrays of fluorocarbon and hydrocarbon tails.

Antiparallel alignment of neighboring molecules is in sharp contrast with the notion of polyphilic ordering—chemically similar parts of amphiphilic molecules associate with one another [9,10]. We note that short chain perfluoroalkanes are partially soluble in their hydrocarbon analogs, with the solubility decreasing with increasing chain length [11,12]. However, the entropy of mixing alone does not account for the highly ordered state observed here. We propose that steric considerations drive the antiparallel alignment of neighboring molecules. Volumetric data from polymers indicate that perfluorinated chains have a cross-sectional area approximately 27% larger than that of hydrocarbon chains [polytetrafluoroethylene (PTFE):polyethylene (PE)=28 Å^2:22 Å^2 [13]]. Antiparallel packing is an efficient way to fill space for $d<1$. Parallel packing would produce a higher energy structure due to local splay of neighboring molecules. This local splay, with associated bend in the smectic layers, is shown in Fig. 3(d).

The semifluorinated *n*-alkanes provide insight regarding the role of the aromatic cores in liquid crystal systems. Two smectic phases are observed in the (C_mF_{2m+1})-(C_nH_{2n+1}) series, where $m=10$ and

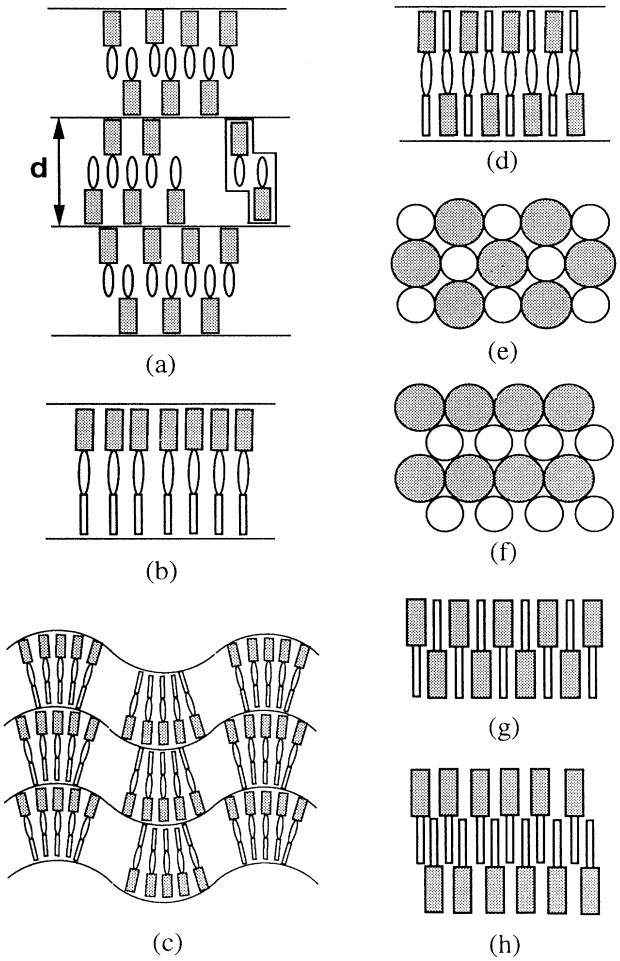

FIG. 3. Various smectic packings in which cores are represented by ovals, and hydrocarbon and fluorinated tails are represented by open and shaded rectangles, respectively. (a) A network in which the smectic layer spacing is independent of hydrocarbon tails. (b) Parallel. (c) A nonpolar organization of parallel aligned molecules. The disparity in the cross-sectional area of the hydrocarbon and fluorocarbon leads to a splayed arrangement and resulting layer bend. (d) Antiparallel alignment of neighboring molecules. (e) and (f) Local in-plane packing structures of rectangular and hexagonal arrays, respectively. Here fluorocarbon tails are represented by shaded circles; hydrocarbon tails by open circles. Intermolecular distances are approximately 5 Å as determined from x-ray scattering from bulk samples in 0.5 mm capillary tubes using the same scattering conditions noted in the text. (g) and (h) Schematic representations of the semifluorinated *n*-alkanes—a similar system, which demonstrates two smectic phases. (g) Antiparallel arrangement of the high temperature phase. (h) Interdigitated structure of the low temperature phase.

$n=9,10,11$ [14–17]. The high temperature phase is analogous to that described here; neighboring molecules within a smectic layer are aligned antiparallel and $d \sim 1$ [Fig. 3(g)]. The low temperature smectic phase is a bilayer structure with $d > 1$, in which the hydrocarbon segments are interdigitated at the center of the layer and the perfluorinated segments are at the layer boundaries [Fig. 3(h)]. The absence of the lower energy interdigitated structure in the liquid crystal system may be accounted for by the energy of association of the core groups. The smectic layer spacing in both phases of the semifluorinated n-alkanes is *dependent* on the length of the fluorocarbon *and* on the length of the hydrocarbon segments [17]. In the liquid crystal system, the smectic layer spacing is *independent* of the hydrocarbon tail length. The aromatic cores of the liquid crystal appear to play a significant role in the registration of neighboring molecules [Fig. 3(a)].

The dimerlike packing described here is unique in two respects. First, the layer spacing is comparable to the molecular length ($d \lesssim 1$). Dimer formation, driven by steric or polar interactions, has been reported for many materials [18–21]. However, in these cases the layer spacing is greater than the molecular length ($1 < d \leq 21$). Second, ferroelectric switching is observed in the Sm-C^* phase of all homologs in Table I when doped with a chiral liquid crystal. Ferroelectric switching has not been reported in other dimerlike forming systems.

V. CONCLUSION

We have discovered unique dimerlike Sm-A and Sm-C phases in a homologous series of rod-shaped, liquid-crystal-forming molecules with one fluorocarbon and one hydrocarbon tail. These materials form a network in which the smectic layer spacing is comparable to the molecular length but is independent of the length of the hydrocarbon tail. Steric interactions dominate the amphiphilic interactions, tending to segregate the fluorocarbon and hydrocarbon tails. Thus, neighboring molecules align antiparallel to one another within a smectic layer. We have shown that the aromatic cores appear significant in the registration of neighboring molecules. The dimerlike packing described here, with $d \lesssim 1$, is a new variation of the Sm-A and Sm-C liquid crystal phases. The observation of ferroelectric switching in the Sm-C^* phase in chiral doped samples is unique among dimerlike forming systems.

ACKNOWLEDGMENTS

We wish to thank C. R. Safinya of the Exxon Research and Engineering Co., Annandale, NJ for providing time on the two-circle x-ray diffractometer; N. A. Clark at the University of Colorado, Boulder, for helpful discussions; and the following people from the 3M Corporation, St. Paul, MN: P. M. Savu, T. D. Spawn, and G. C. Johnson for materials synthesis, and P. Leung for molecular length calculations. This work was supported by Los Alamos and Sandia National Laboratories (operated for the U.S. Department of Energy under Contract Nos. W-7405-ENG-36 and DE-AC04-94AL85000, respectively) and the 3M Corporation.

[1] E. P. Janulis, J. C. Novack, G. A. Papapolymerou, M. Tristan-Kendra, and W. A. Huffman, Ferroelectrics **85**, 375 (1988).
[2] E. P. Janulis, U.S. Patent No. 4,886,619 (1989).
[3] E. P. Janulis, U.S. Patent No. 5,082,587 (1992).
[4] E. P. Janulis, D. W. Osten, M. D. Radcliffe, J. C. Novack, M. Tristani-Kendra, K. A. Epstein, M. Keyes, G. C. Johnson, P. M. Savu, and T. D. Spawn, Proc. Soc. Photo-Opt. Instrum. Eng. **1665**, 143 (1992).
[5] R. B. Meyer, L. Liebert, L. Strezelecki, and P. Keller, J. Phys. (Paris) Lett. **36**, L69 (1975).
[6] R. Kiefer and G. Baur, Liq. Cryst. **7**, 815 (1990).
[7] S. Kumar, Phys. Rev. A **23**, 3207 (1981).
[8] J. J. P. Stewart, MOPAC Version 6, QCPE No. 455 **10**, 86 (1990).
[9] F. Tournilhac, L. Bosio, J.-F. Nicoud, and J. Simon, Chem. Phys. Lett. **145**, 452 (1988).
[10] F. Tournilhac and J. Simon, Ferroelectrics **114**, 283 (1991).
[11] R. L. Scott, J. Phys. Chem. **62**, 136 (1958).
[12] C. L. Young, Trans. Faraday Soc. **65**, 2639 (1969).
[13] *Polymer Handbook,* edited by J. Brandup and E. H. Immergut (Wiley, New York, 1975).
[14] C. Viney, T. P. Russell, L. E. Depero, and R. J. Twieg, Mol. Cryst. Liq. Cryst. **168**, 63 (1989).
[15] C. Viney, R. J. Twieg, T. P. Russell, and L. E. Depero, Liq. Cryst. **5**, 1783 (1989).
[16] J. Höpken and M. Möller, Macromolecules **25**, 2482 (1992).
[17] J. F. Rabolt, T. P. Russell, and R. J. Twieg, Macromolecules **17**, 2786 (1984).
[18] A. J. Leadbetter, J. C. Frost, J. P. Gaughan, and G. W. Gray, J. Phys. (Paris) **40**, 375 (1979).
[19] E. Fanelli, G. Poeti, G. Albertini, O. Francescangeli, R. Torquati, and P. Mariani, Nuovo Cimento D **12**, 69 (1990).
[20] F. Hardouin, M. F. Achard, C. Destrade, and Nguyen Huu Tinh, J. Phys. (Paris) **45**, 765 (1984).
[21] W. H. deJeu, in *Phase Transitions in Liquid Crystals* Vol. 290 of *NATO Advanced Study Institute, Series B: Physics,* edited by S. Martellucci and A. N. Chester (Plenum, New York, 1992).